

The importance of metal–support interactions for CO₂ hydrogenation: An operando NAP-XPS study on gold-loaded In₂O₃ and CeO₂ catalysts

Marc Ziemba¹, Jakob Weyel¹, Patrick Zeller^{2,3}, Jan Welzenbach¹, Anna Efimenko^{4,5}, Michael Hävecker^{3,6}, and Christian Hess^{1*}

¹Eduard Zintl Institute of Inorganic and Physical Chemistry, Technical University of Darmstadt, Peter-Grünberg-Str. 8, 64287 Darmstadt, Germany

²Helmholtz-Zentrum Berlin für Materialien und Energie GmbH (HZB), BESSY II, Albert-Einstein-Str. 15, 12489 Berlin, Germany

³Department of Inorganic Chemistry, Fritz-Haber-Institut der Max-Planck-Gesellschaft, Faradayweg 4-6, 14195 Berlin, Germany

⁴Interface Design, Helmholtz-Zentrum Berlin für Materialien und Energie GmbH (HZB), Albert-Einstein-Str. 15, 12489 Berlin, Germany

⁵Energy Materials In-situ Laboratory Berlin (EMIL), HZB, Albert-Einstein-Str. 15, 12489 Berlin, Germany

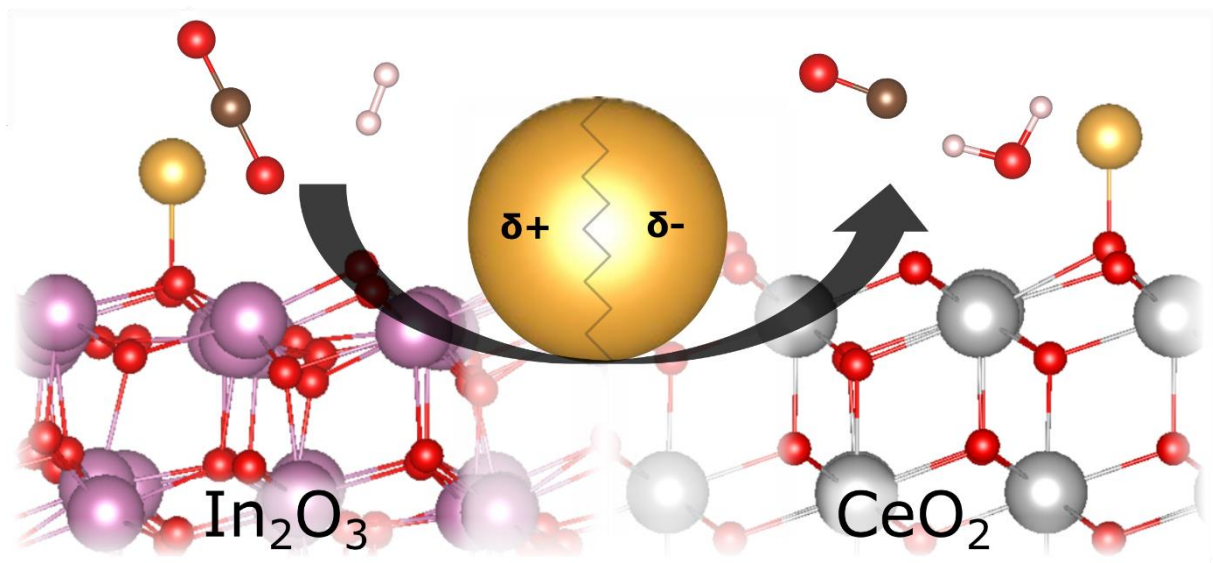
⁶Department of Heterogeneous Reactions, Max Planck Institute for Chemical Energy Conversion, Stiftstrasse 34-36, 45470 Mülheim an der Ruhr, Germany

*email: christian.hess@tu-darmstadt.de

Keywords

NAP-XPS, CO₂ hydrogenation, gold, CeO₂, In₂O₃, metal–support interaction

Graphical Abstract



Abstract (150 words max)

Metal–support interactions, which are essential for the design of supported metal catalysts, used e.g. for CO₂ activation, are still only partially understood. In this study of gold-loaded In₂O₃ and CeO₂ catalysts during CO₂ hydrogenation using near ambient pressure XPS (NAP-XPS), supported by NEXAFS, we demonstrate that the role of the noble metal strongly depends on the choice of the support material. Temperature-dependent analyses of XP spectra under reaction conditions reveal that gold is reduced on CeO₂, enabling direct H₂ activation, but oxidized on In₂O₃, leading to decreased activity of Au/In₂O₃ compared to bare In₂O₃. At elevated temperatures, the catalytic activity of the In₂O₃ catalysts strongly increases due to facilitated CO₂ and (In₂O₃-based) H₂ activation while the catalytic activity of Au/CeO₂ is limited by reoxidation by CO₂. Our results underline the importance of operando studies for understanding metal–support interactions to enable a rational support selection in the future.

In the context of the energy transition and to mitigate climate change, the use of CO₂ as a non-fossil carbon source is an important option for the production of chemicals and fuels. It has been shown that CO₂ activation is facilitated by heterogeneous catalysts based on reducible oxides such as In₂O₃ and CeO₂ due to their excellent redox properties.^[1–4] As a result, lattice oxygen can be provided for reactions in which oxygen is involved, such as CO oxidation,^[5] the (reverse) water–gas shift reaction,^[6–10] and CO₂ hydrogenation to methanol.^[11,12] Regarding the redox properties of CeO₂ and In₂O₃, cerium can easily switch its oxidation state between Ce³⁺ and Ce⁴⁺,^[9] whereas the oxidation state of indium was observed to change between In³⁺ and metallic In⁰.^[13] In the context of catalysis, where these reducible oxides are often loaded with metals (e.g. Pt, Au, Cu), another property of key importance is the metal–support interaction.^[14]

^{16]} The reason for this is that in many cases the metal particles on the oxide or their interface constitute the active site,^[17] which in turn is strongly influenced by the transfer of electrons between the metal and the support. Furthermore, the metal can have an influence on the defect formation energy.

In this study, we compare the mechanistic behavior of gold-loaded In₂O₃ and CeO₂ catalysts during CO₂ hydrogenation to CO and water, that is, the reverse water–gas shift reaction (rWGSR). Both catalysts have shown good rWGSR activity in past studies,^[3,7] but a direct comparison between the two metal oxides regarding the gold state and the different influence of the support on the metal under reaction conditions has not been reported. Moreover, despite its relevance for heterogeneous catalysis in general, the effect of the metal–support interaction on the catalysis during CO₂ hydrogenation (rWGSR) has not been clarified yet. In this letter, we address this point based on gold catalysts, underlining its importance and providing an impulse for its more detailed consideration in future studies.

In₂O₃ and CeO₂ were synthesized as described in our previous studies^[7,8] and loaded with gold using the deposition–precipitation method.^[18] The gold loadings were validated by ICP-OES (inductively coupled plasma optical emission spectrometry) as 1.03 wt% for In₂O₃ and 1.05 wt% for CeO₂. The specific surface areas according to N₂ adsorption and the BET model for the bare supports are 57 m²/g for CeO₂ and 39 m²/g for In₂O₃. The samples were then studied in more detail using operando near ambient pressure X-ray photoelectron spectroscopy (NAP-XPS), experimental details of which can be found in the Supporting Information (SI). For the Au/ceria, operando near-edge X-ray absorption fine structure (NEXAFS) measurements of the Ce L₃-edge and the M_{4,5}-edges were also conducted (see SI for details). The samples were analyzed at 1 mbar total pressure of H₂ and CO₂, using flow rates of 6.66 ml/min and 3.33 ml/min, respectively. Three different temperatures were successively considered, that is, 200, 250, and 300 °C.

The catalytic activity during rWGSR was monitored by gas chromatography (for details see SI).

Carbon monoxide and water were the only detected products. Neither sample is active at 200 °C. At 250 °C Au/In₂O₃ shows a CO₂ conversion of 0.026% and Au/CeO₂ a CO₂ conversion of 0.045%, and at 300 °C the conversions are 0.128 and 0.094%, respectively. Thus, at 250 °C, the ceria-based catalyst is slightly more active than Au/In₂O₃, whereas at 300 °C, the latter shows a higher activity. For comparison, bare CeO₂ showed no activity, while In₂O₃ is active with CO₂ conversions of 0.080% and 0.180% at 250 and 300 °C, respectively, which are higher than those of the gold-loaded In₂O₃. The conversions appear to be low, but can be rationalized by the low pressure of the operando setup. The latter also prevents the formation of methanol during CO₂ hydrogenation. Summarizing the activity results, we can state that the effect of the gold loading strongly depends on the choice of the support material.

To gain insight into the observed reactivity behavior, we used NAP-XPS under reaction conditions. First, the gold state will be examined in more detail based on the Au 4f photoemission of the two samples at different temperatures under reaction conditions, as shown in Figure 1. It is apparent that the Au 4f signal of the CeO₂ sample is located at lower binding energy than that of the In₂O₃ sample (see also SI). This behavior indicates that gold behaves differently on the two different oxide supports and is more oxidized on In₂O₃. Moreover, when considering the different temperatures, it can be seen that for the In₂O₃-based sample the Au 4f signal shifts to higher binding energies with increasing temperature, while the Au/CeO₂ sample shows the opposite behavior. Thus, gold on In₂O₃ is oxidized with increasing temperature, while it is reduced on CeO₂, evidencing a clear difference in the behavior of gold on the two support materials, which may be associated with different metal–support interactions.

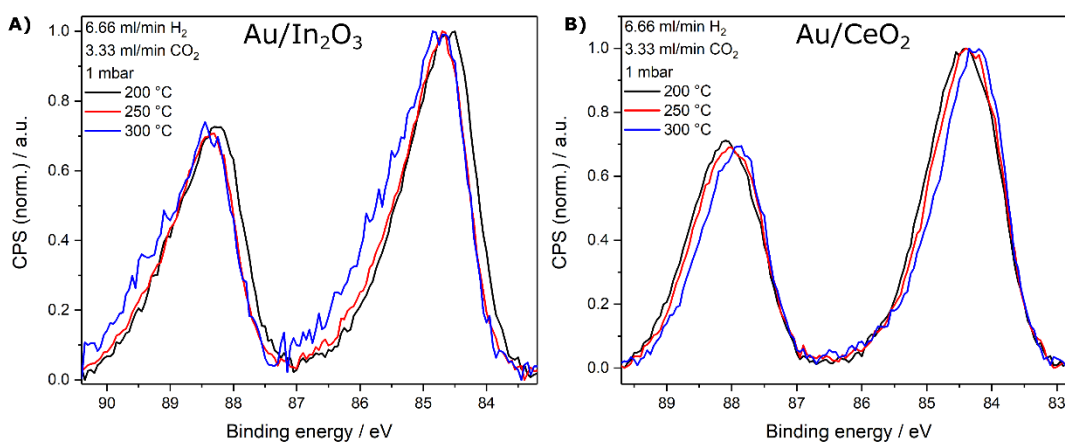


Figure 1: Au 4f photoemission of **A)** gold-loaded In_2O_3 and **B)** gold-loaded CeO_2 during rWGS. Operando spectra were recorded at a total pressure of 1 mbar, composed of H_2 (6.66 ml/min) and CO_2 (3.33 ml/min), at 200 °C (black), 250 °C (red), and 300 °C (blue).

Next, the spectra of the In 3d and Ce 3d regions of the gold-loaded In_2O_3 and CeO_2 samples will be considered (see Figure 2). As expected for In_2O_3 , based on the In $3d_{5/2}$ binding energy (BE), indium is present in the oxidation state In^{3+} at 200 °C and no significant change takes place with the onset of the reaction at higher temperatures. Thus, we can conclude that the oxidation state of indium at the surface does not change significantly. To support this finding, the In MNN region was measured (see Figure S1), which did not show any changes in oxidation state either, as neither a significant shift in the binding energy nor a change in the band shape was observed.^[19] In contrast, in the case of CeO_2 , Ce^{3+} is already present on the surface from the beginning, besides Ce^{4+} (see Figure 2B), and it increases in concentration with increasing temperature, indicating the formation of oxygen defects. This increase in Ce^{3+} concentration also correlates with the catalytic activity. For cerium, we could perform additional NEXAFS measurements, where the total electron yield (TEY) was detected, giving rise to a slightly higher penetration depth compared to the XPS measurements. Based on the Ce L_3 edge and the Ce $M_{4,5}$ edges (see Figures S2 and S3), an increase of the Ce^{3+} fraction is observed, strongly suggesting that the sub-surface is also participating in the reaction.^[20] Thus, comparison of the behavior of CeO_2 and In_2O_3 reveals that the CeO_2 support is significantly

involved in the reaction, while In_2O_3 does not undergo any changes in oxidation state. To gain further mechanistic insight, the surface oxygen dynamics was analyzed as a function of temperature.

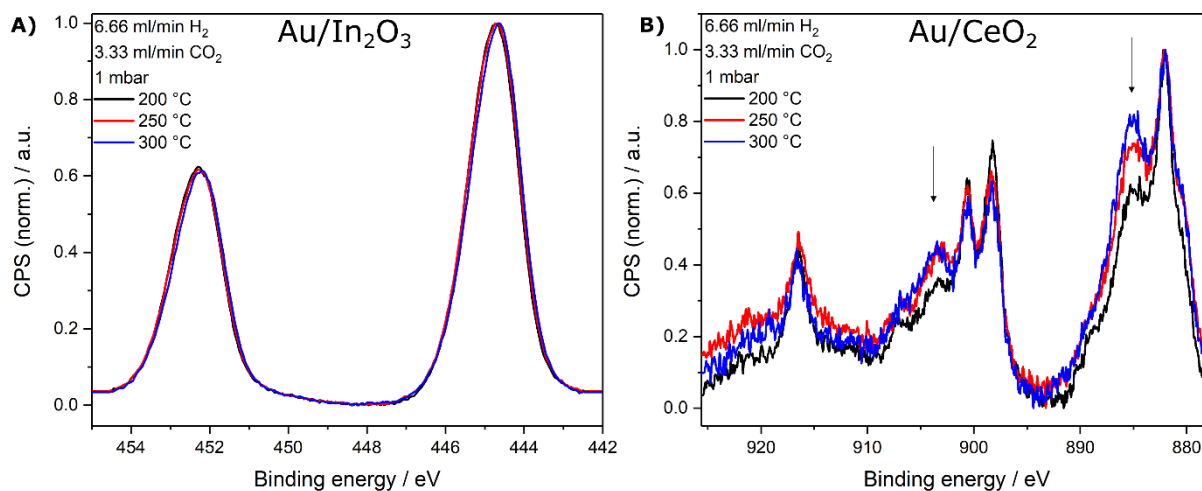


Figure 2: A) In 3d photoemission of gold-loaded In_2O_3 and B) Ce 3d photoemission of gold-loaded CeO_2 during rWGS. Operando spectra were recorded at a total pressure of 1 mbar, composed of H_2 (6.66 ml/min) and CO_2 (3.33 ml/min), at 200 °C (black), 250 °C (red), and 300 °C (blue). The Ce^{3+} contributions are indicated by the black arrows.

Figure 3 depicts the O 1s spectra of Au/ In_2O_3 (see Figure 3A) and Au/ CeO_2 (see Figure 3B). It can readily be seen that the O 1s signals of the two oxides are characterized by a different spectral profile and temperature-dependent behavior. In fact, the O 1s feature is much broader for CeO_2 than for In_2O_3 , with at least four distinct contributions for CeO_2 . In contrast, for In_2O_3 , the overall changes are less pronounced, and with increasing temperature mainly a decrease of the width and the asymmetry of the band is observed, suggesting that all contributions decrease, except that from lattice oxygen.^[21,22] According to the literature on In_2O_3 , the signal at 529.9 eV originates from lattice oxygen, while defective indium oxide gives rise to a signal at around 531 eV. The component at around 532 eV has been attributed to surface hydroxides^[23] with a possible contribution from carbonates.^[21,23] Figure 3A shows both the hydroxide-/carbonate- and defect-related signals decrease with increasing temperature. This behavior is consistent

with UV/Vis results from our earlier study, which showed that, starting at about 220 °C, the surface was increasingly oxidized by CO₂ under reaction conditions as the temperature was increased.^[8]

For the CeO₂ sample, the highest energy O 1s contribution is located at about 533.5 eV, which is typical of adsorbed H₂O.^[24] The two features at around 531.7 and 530.6 eV have been assigned to hydroxide groups and defective ceria (lattice oxygen bound to Ce³⁺), respectively. The signal at 529.5 eV originates from lattice oxygen bound to Ce⁴⁺.^[24,25] It can be seen that the hydroxide signal remains approximately the same when the temperature is raised to 250 °C, whereas at 300 °C, the hydroxide signal clearly declines. On the other hand, the 530.6 eV feature first increases but then remains about the same at 300 °C, indicating that the number of oxygen defects significantly increases above 250 °C, which is consistent with the Ce 3d photoemission (see Figure 2B) but contrary to the behavior observed for In₂O₃. In addition, it is worth mentioning that for both oxides the signal at 533.5 eV, indicating water formation, is detected only at higher temperatures and is consistent with the activity measurements using gas chromatography (GC). Please note that in the case of In₂O₃, the 533.5 eV signal becomes visible only at 300 °C, which can be attributed either to the lower conversion of In₂O₃ at 250 °C or to the fact that more water is formed at 300 °C, because of the higher activity.

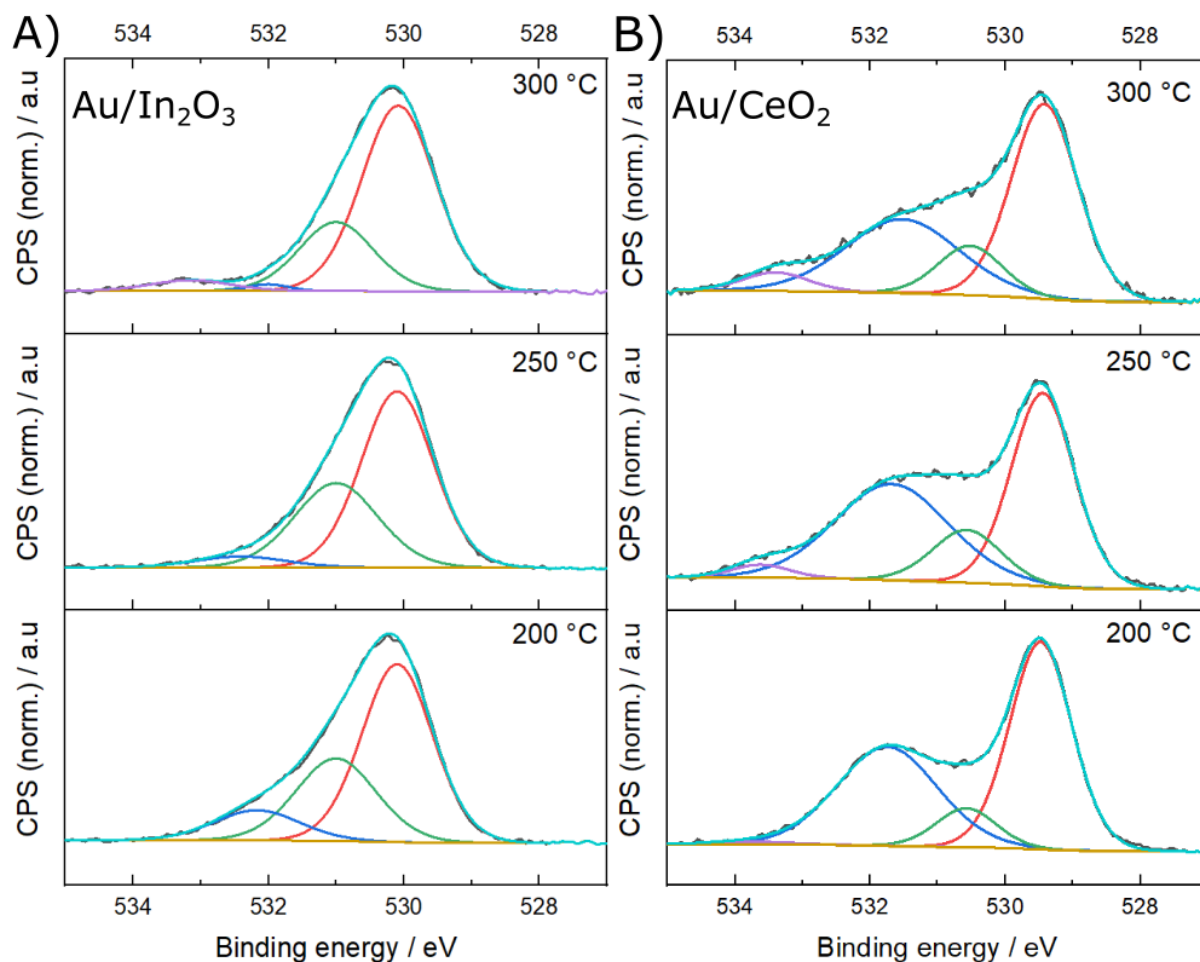


Figure 3: O 1s photoemission of **A)** gold-loaded In₂O₃ and **B)** gold-loaded CeO₂ during rWGS. Operando spectra were recorded at a total pressure of 1 mbar, composed of H₂ (6.66 ml/min) and CO₂ (3.33 ml/min), at 200 °C, 250 °C and 300 °C. The O1s signal from the defect-free oxide is shown in red, near defects in green, that of hydroxides in blue and that of adsorbed water in purple.

To explore whether adsorbates such as formates or carbonates are also involved, we analyzed the C 1s spectra (see Figure S4). For both oxides, a carbonate-related signal at 289.3 eV was detected, which disappears with increasing temperature. These carbonates are presumably present on the powders from the beginning, originating from atmospheric CO₂. The observed desorption behavior makes their involvement in the reaction unlikely. Furthermore, the center of the C 1s signal seems to show a red-shift with increasing temperature, but this is

related to the desorption of carbon-containing adsorbates instead of a change in the ubiquitous carbon signal.

In summary, in this operando NAP-XPS study, we explored the interaction between gold and the supporting oxide and how this affects the reactivity behavior, including the role of the gold and cerium oxidation states. Our results show that the gold is more positively charged on In_2O_3 , which prevents adsorption/activation of H_2 . In contrast, such a H_2 activation has been demonstrated for Au/CeO_2 in one of our previous studies using transient IR spectroscopy and density functional theory (DFT) calculations.^[7] Thus, we propose that gold plays no essential role in H_2 activation on In_2O_3 , and that H_2 is rather activated by the oxide. This is also reflected in the activity of the gold-loaded In_2O_3 , which has a slightly lower activity than without gold. The more positive Au charge on In_2O_3 may be explained by the fact that In_2O_3 activates more CO_2 at higher temperatures and thus becomes more oxidized, thereby increasing the availability of lattice oxygen for oxidizing the gold. This is not the case for CeO_2 , which transforms into a more reduced state with increasing temperature.

The oxidation of indium oxide by CO_2 has been demonstrated in previous studies, using, for example, temperature-dependent operando UV/Vis spectroscopy,^[8] which is a more bulk-sensitive method than XPS. Comparing this study to our earlier findings reveals that the surface is also involved in the oxidation process, since operando NAP-XPS detects a decrease in the number of oxygen defects with increasing temperature. Indium itself is not subject to any surface reduction within the sensitivity of XPS, because this would be indicated by a change of the In MNN signal profile and a shift in the In 3d position.

Thus, based on the available data, we propose that reduction of the $\text{Au}/\text{In}_2\text{O}_3$ catalyst by H_2 is activated by In_2O_3 that is largely unaffected by the presence of Au. On the other hand, the surface hardly reacts with CO_2 at still moderate conditions. Only with increasing temperature, can CO_2 finally be activated, leading to surface reoxidation. Compared to the Au/CeO_2 catalyst, the reaction proceeds much more slowly at 250 °C, because on the Au/CeO_2 surface H_2 is

activated by gold even at moderate conditions and, as a consequence, the surface is reduced. However, while H₂ activation is facilitated by Au, the reoxidation by CO₂ proceeds much more slowly, thus limiting the catalytic activity at 300 °C, as evidenced by the increase in surface reduction with increasing temperature.

In this study, we provide direct experimental evidence that the influence of the noble metal on the reactivity behavior is strongly dependent on the support. As shown for supported Au catalysts during CO₂ activation, the use of In₂O₃ and CeO₂ as reducible oxide supports leads to a completely different behavior of the loaded gold. This ranges from direct H₂ activation on CeO₂ to a deactivation on In₂O₃, which is probably linked to the blocking of active sites, leading to a decreased activity of Au/In₂O₃ compared to bare In₂O₃. Our results highlight the importance of operando studies for understanding metal–support interactions and their relevance for the reactivity behavior of loaded oxide catalysts, enabling a rational support selection in the future.

Acknowledgements

We thank the Helmholtz-Zentrum Berlin (HZB) für Materialien und Energie for the allocation of synchrotron radiation beamtime at the CAT branch of the Energy Materials In-Situ Laboratory Berlin (EMIL). We thank Mihaela Gorgoi (HZB) for the EMIL beamline support and maintenance.

Supporting Information

Detailed information on experimental methods as well as additional experimental data.

References

- [1] Hinuma, Y.; Toyao, T.; Hamamoto, N.; Takao, M.; Shimizu, K. I.; Kamachi, T. Changes in Surface Oxygen Vacancy Formation Energy at Metal/Oxide Perimeter Sites: A Systematic Study on Metal Nanoparticles Deposited on an In₂O₃(111) Support. *J. Phys. Chem. C* **2020**, *124*, 27621 – 27630.
- [2] Pinheiro Araújo, T.; Morales-Vidal, J.; Zou, T.; García-Muelas, R.; Willi, P. O.; Engel, K. M.; Safonova, O. V.; Faust Akl, D.; Krumeich, F.; Grass, R. N.; Mondelli, C.; López, N.; Pérez-Ramírez, J. Flame Spray Pyrolysis as a Synthesis Platform to Assess Metal Promotion in In₂O₃-Catalyzed CO₂ Hydrogenation. *Adv. Energy Mater.* **2022**, *12*, 2103707.
- [3] Rui, N.; Zhang, F.; Sun, K.; Liu, Z.; Xu, W.; Stavitski, E.; Senanayake, S. D.; Rodriguez, J. A.; Liu, C.-J. Hydrogenation of CO₂ to Methanol on a Au^{δ+}-In₂O_{3-x} Catalyst. *ACS Catal.* **2020**, *10*, 11307–11317.
- [4] Rui, N.; Sun, K.; Shen, C.; Liu, C.-J. Density functional theoretical study of Au₄/In₂O₃ catalyst for CO₂ hydrogenation to methanol: The strong metal-support interaction and its effect. *J. CO₂ Util.* **2020**, *42*, 101313.
- [5] Ziemba, M.; Hess, C.; Influence of gold on the reactivity behaviour of ceria nanorods in CO oxidation: combining operando spectroscopies and DFT calculations. *Catal. Sci. Technol.* **2020**, *10*, 3720–3730.
- [6] Ziemba, M.; Weyel, J.; Hess, C. Approaching C1 Reaction Mechanisms Using Combined *Operando* and Transient Analysis: A Case Study on Cu/CeO₂ Catalysts during the LT-Water-Gas Shift Reaction. *ACS Catal.* **2022**, *12*, 9503–9514.
- [7] Ziemba, M.; Weyel, J.; Hess, C. Elucidating the mechanism of the reverse water-gas shift reaction over Au/CeO₂ catalysts using *operando* and transient spectroscopies. *Appl. Catal. B* **2022**, *301*, 120825.
- [8] Ziemba, M.; Radtke, M.; Schumacher, L.; Hess, C. Elucidating CO₂ Hydrogenation over In₂O₃ Nanoparticles using Operando UV/Vis and Impedance Spectroscopies. *Angew. Chem. Int. Ed.* **2022**, *61*, e202209388.
- [9] Ziemba, M.; Schilling, C.; Ganduglia-Pirovano, M. V.; Hess, C. Toward an Atomic-Level Understanding of Ceria-Based Catalysts: When Experiment and Theory Go Hand in Hand. *Acc. Chem. Res.* **2021**, *54*, 2884–2893.

- [10] Ziemba, M.; Hess, C. Unravelling the mechanism of CO₂ activation over low-loaded Cu/CeO₂(111) catalysts using operando and transient spectroscopies. *Catal. Sci. Technol.* **2023**, *13*, 2922–2926.
- [11] Zhu, J.; Su, Y.; Chai, J.; Muravev, V.; Kosinov, N.; Hensen, E. J. M. Mechanism and Nature of Active Sites for Methanol Synthesis from CO/CO₂ on Cu/CeO₂. *ACS Catal.* **2020**, *10*, 11532–11544.
- [12] Ghosh, S.; Sebastian, J.; Olsson, L.; Creaser, D. Experimental and kinetic modeling studies of methanol synthesis from CO₂ hydrogenation using In₂O₃ catalyst. *Chem. Eng. J.* **2021**, *416*, 129120.
- [13] Bielz, T.; Lorenz, H.; Jochum, W.; Kaindl, R.; Klauser, F.; Klötzer, B.; Penner, S. Hydrogen on In₂O₃: Reducibility, Bonding, Defect Formation, and Reactivity. *J. Phys. Chem. C* **2010**, *114*, 9022–9029,
- [14] Fu, Q.; Saltsburg, H.; Flytzani-Stephanopolous, M. Active Nonmetallic Au and Pt Species on Ceria-Based Water-Gas Shift Catalysts. *Science* **2003**, *301*, 935–938.
- [15] Widmann, D.; Behm, R. Active Oxygen on a Au/TiO₂ Catalyst: Formation, Stability, and CO Oxidation Activity. *Angew. Chem. Int. Ed.* **2011**, *50*, 10241–10245.
- [16] Li, Y.; Kottwitz, M.; Vincent, J. L.; Enright, M. J.; Liu, Z.; Zhang, L.; Huang, J.; Senanayake, S. D.; Yang, W.-C. D.; Crozier, P. A.; Nuzzo, R. G.; Frenkel, A. I., Dynamic structure of active sites in ceria-supported Pt catalysts for the water gas shift reaction. *Nature Commun.* **2021**, *12*, 914.
- [17] Weyel, J.; Ziemba, M.; Hess, C. Elucidating Active CO–Au Species on Au/CeO₂(111): A Combined Modulation Excitation DRIFTS and Density Functional Theory Study. *Top. Catal.* **2022**, *65*, 779–787.
- [18] Schilling, C.; Hess, C. CO Oxidation on Ceria Supported Gold Catalysts Studied by Combined *Operando* Raman/UV–Vis and IR Spectroscopy. *Top. Catal.* **2017**, *60*, 131–140.
- [19] Rossnagel, S. M.; Dylla, H. F.; Cohen, S. A. AES study of the adsorption of O₂, CO, CO₂, and H₂O on indium. *J. Vac. Sci. Technol.* **1979**, *16*, 558–561.
- [20] Kucheyev, S. O.; Clapsaddle, B. J.; Wang, Y. M.; van Buuren, T.; Hamza, A. V. Electronic structure of nanoporous ceria from x-ray absorption spectroscopy and atomic multiplet calculations. *Phys. Rev. B* **2007**, *76*, 235420.

- [21] Li, M.; Luo, W.; Züttel, A. Near ambient-pressure X-ray photoelectron spectroscopy study of CO₂ activation and hydrogenation on indium/copper surface. *J. Catal.* **2021**, *395*, 315–324.
- [22] Wang, Y.; Zhu, L.; Liu, Y.; Vovk, E. I.; Lang, J.; Zhou, Z.; Gao, P.; Li, S.; Yang, Y. Understanding surface structures of In₂O₃ catalysts during CO₂ hydrogenation reaction using time-resolved IR, XPS with *in situ* treatment, and DFT calculations. *Appl. Surf. Sci.* **2023**, *631*, 157534.
- [23] Hoch, L. B.; He, L.; Qiao, Q.; Liao, K.; Reyes, L. M.; Zhu, Y.; Ozin, G. A. Effect of Precursor Selection on the Photocatalytic Performance of Indium Oxide Nanomaterials for Gas-Phase CO₂ Reduction. *Chem. Mater.* **2016**, *28*, 4160–4168.
- [24] Li, Z.; Werner, K.; Qian, K.; You, R.; Płucienik, A.; Jia, A.; Wu, L.; Zhang, L.; Pan, H.; Kuhlenbeck, H.; Shaikhutdinov, S.; Huang, W.; Freund, H. Oxidation of Reduced Ceria by Incorporation of Hydrogen. *Angew. Chem. Int. Ed.* **2019**, *58*, 14686–14693.
- [25] Patra, K. K.; Liu, Z.; Lee, H.; Hong, S.; Song, H.; Abbas, H. G.; Kwon, Y.; Ringe, S.; Oh, J. Boosting Electrochemical CO₂ Reduction to Methane via Tuning Oxygen Vacancy Concentration and Surface Termination on a Copper/Ceria Catalyst. *ACS Catal.* **2022**, *12*, 10973–10983.